Received: 6 December 2018 | Accepted: 27 December 2018
DOI: 10.1002/pros.23764

ORIGINAL ARTICLE

WILEY The Prostate

Nanoscale flow cytometry to distinguish subpopulations of prostate extracellular vesicles in patient plasma

Ranjit S. Padda MSc[1,2] | Florence K. Deng MD[1,2] | Sabine I. Brett MSc[1,2] | Colleen N. Biggs BSc[3] | Paul N. Durfee PhD[3] | Charles J. Brinker PhD[3] | Karla C. Williams PhD[1] | Hon S. Leong PhD[1,2]

[1] Translational Prostate Cancer Research Laboratory, Lawson Health Research Institute, London, Ontario

[2] Department of Surgery, Schulich School of Medicine and Dentistry, Western University, London, Ontario

[3] Sandia National Laboratories, Albuquerque, New Mexico

Correspondence
Hon S. Leong, MSc, PhD, Translational Prostate Cancer Research Laboratory, Lawson Health Research Institute, F3-117, St. Joseph's Hospital, 268 Grosvenor St. London, London N6A 4V2, ON.
Email: honsing.leong@gmail.com

Funding information
Prostate Cancer Fight Foundation; Prostate Cancer Canada, Grant numbers: Pilot Grant 2012, RS2012-008, RS2016-56

Objective: To determine if prostate-derived extracellular vesicles (EVs) present in patient plasma samples are of exocytotic origin (exosomes) or released by the cell membrane (microparticles/microvesicles). Both malignant and normal prostate cells release two types of EVs into the circulation, exosomes, and microparticles/microvesicles which differ in size, origin, and mode of release. Determining what proportion of prostate-derived EVs are of exosomal versus microparticle/microvesicle EV subtype is of potential diagnostic significance.

Materials and Methods: Multi-parametric analytical platforms such as nanoscale flow cytometry (nFC) were used to analyze prostate derived extracellular vesicles. Plasmas from prostate cancer (PCa) patient plasmas representing benign prostatic hyperplasia (BPH), low grade prostate cancer (Gleason Score 3 + 3) and high grade prostate cancer (Gleason Score ≥4 + 4) were analyzed for various exosome markers (CD9, CD63, CD81) and a prostate specific tissue marker (prostate specific membrane antigen/PSMA).

Results: By using nanoscale flow cytometry, we determine that prostate derived EVs are primarily of cell membrane origin, microparticles/microvesicles, and not all PSMA expressing EVs co-express exosomal markers such as CD9, CD63, and CD81. CD9 was the most abundant exosomal marker on prostate derived EVs (12-19%). There was no trend observed in terms of more PSMA + CD9 or PSMA + CD63 co-expressing EVs versus increasing grade of prostate cancer.

Conclusion: The majority of prostate derived EVs present in plasmas are from the cell membrane as evidenced by their size and most importantly, lack of co-expression of exosomal markers such as CD9/CD63/CD81. In fact, CD81 was not present on any prostate derived EVs in patient plasmas whereas CD9 was present on a minority of prostate derived EVs. The addition of an exosomal marker for detection of prostate-derived EVs does not provide greater clarity in distinguishing EVs released by the prostate.

KEYWORDS
benign prostatic hyperplasia, CD63, CD9, exosomes, extracellular vesicles, nanoscale flow cytometry, prostate cancer, PSMA

1 | INTRODUCTION

The primary function of the prostate gland is the synthesis and secretion of various proteins and proteases into human seminal fluid, conferring important protective effects for sperm post-ejaculation. The prostate also releases extracellular vesicles, originally termed prostasomes,[1] into seminal fluid and these storage vesicles also contain key constituents of seminal fluid.[2] Extracellular vesicles (EVs) can arise via fragmentation or "budding" of the cell membrane, are 100-1000 nm in diameter, and are known as microparticles/microvesicles.[3,4] Alternatively, they can also arise via exocytosis of endosomal vesicles or storage vesicles, are 50-150 nanometers in diameter, and are known as exosomes.[4] It is unclear whether prostasomes are formed exclusively through either mechanism or a mixture of both mechanisms, with some indications that prostasomes are morphologically more similar to exosomes and generated via exocytosis.[1] Furthermore, the existence of two different types of exosomes in seminal fluid, between 40 and 70 nm and 80-130 nm in diameter implicates overlooked complexities in EV biogenesis that occur in prostatic epithelium[5,6] regardless of neoplasia or hyperplasia.[7] Several cell surface antigens such as CD9, CD63, CD81 have been designated as consensus exosome markers with a large set of other proteins known to be enriched within exosomes (exocarta.org) with content varying due to source and sample type.[8–10]

Prostate-derived EVs such as prostasomes which are present in seminal fluid have emerged as a next-generation biomarker platform for prostate-related disorders, supported by recent reports of their abundance in patient urine and blood (plasma/serum) as analyzed by both conventional methods and novel means.[11,12] These prostate-derived EVs and their putative portfolio of biomarkers could be used in distinguishing patients with benign prostatic hyperplasia (BPH), from low-risk prostate cancer (PCa), intermediate-risk PCa, and high-risk PCa.[13,14] Given that serum levels of prostate specific antigen (PSA/KLK3) are elevated in the majority of these patients and undetectable in healthy volunteers,[15,16] it is conceivable that release of prostate-derived EVs into the blood circulation could represent a non-invasive "liquid biopsy" of the prostate for risk stratification of PCa patients. However, this prostate "liquid biopsy" must rely on tissue-specific markers or antigens such as prostate specific membrane antigen (PSMA/FOLH1) as opposed to exosome markers such as CD9, CD63, CD81 because of their expression on other non-prostate derived exosomes, which may be in orders of magnitude more abundant than prostasomes in patient blood.

Recent evidence confirms that PSMA is a suitable tissue-specific antigen for prostasomes,[4,8,9] but our recent work has shown that PSMA + ve EVs in various PCa patient plasmas range from 100 to 500 nanometers in diameter as determined by nanoscale flow cytometry, covering both exosomes and larger EVs such as microparticles/microvesicles. It is possible that a subpopulation of PSMA + ve EVs are of exosomal origin because of their size range between 50 and 150 nm, of which the 100-150 nm size range is covered by nanoscale flow cytometry (nFC, 100-1400 nm).[17] It is also possible that larger EVs (>150 nm in diameter) such as microparticles/microvesicles may also express exosomal markers. Understanding the origin and distinction of prostate-derived EVs in patient blood as being either exosomes versus microparticles/microvesicles is important because their effectiveness as a biomarker platform is dependent on their origin. For example, if a significant proportion of PSMA + ve EVs are exosomes, then techniques such as RNA-seq are more relevant due to their propensity for carrying and off-loading nucleic acid biomarkers such as microRNA and mRNA.[18,19] However, if the majority of PSMA + ve EVs are microparticles/microvesicles, then protein-based techniques would be more relevant for the enumeration of biomarker-laden EVs generated from the prostate and its resident cancer.

Currently, there are two main attributes that distinguish exosomes from microparticles/microvesicles: size and the expression of exosome-specific antigens such as CD9/CD63/CD81. Based on our preliminary data, PSMA + ve EVs cover the full range of sizes (100-1000 nm), with the median diameter size of ~200 nanometers, which is beyond the upper size limit of exosomes.[10,20] Given their larger size, we hypothesized that PSMA + ve EVs in plasma are predominantly larger EVs such as microparticles/microvesicles and do not express consensus exosome markers CD9, CD63, and CD81. To test this, nanoscale flow cytometry was used which enables quantitative, multi-parametric analysis of PSMA + ve EVs for the co-expression of CD9/CD63/CD81 on the surface of individual EVs from patient plasma samples. This evaluation is not currently possible with any other technique such as ELISA, western immunoblotting, electron microscopy, or dynamic light scattering (DLS) methods. Equally important is the ability to perform high-throughput analyses of >500 000 events per flow cytometry run in order to adequately power these studies. In this report, we perform nanoscale flow cytometry on various patient plasma samples representing BPH, low-/intermediate-/high-risk prostate cancer, and determine that the prostate is predominantly releasing prostate microparticles/microvesicles and not exosomes into the blood circulation.

2 | MATERIALS AND METHODS

2.1 | Plasma preparation and ethics

Plasma samples from prostate cancer (PCa) patients were provided by the Ontario Institute for Cancer Research Tumor Bank and the University Health Network Genitourinary BioBank (Toronto, ON) under Western University Research Ethics Board (REB) approved Ethics permits 103156 and 103409. Samples from patients with at least 3 years' follow-up were used in order to avoid patients that upstaged/upgraded prior to analysis by nFC. As per Biobank SOPs, plasma was obtained by processing patient whole blood that was collected in K2 EDTA Vacutainers (BD Biosciences, San Jose, CA; CA# 366643) and centrifuged at 1500*g*'s for 20 min. The plasma supernatant layer was removed, aliquoted, and then stored at −80°C.

2.2 | Reagents for calibration of nanoscale flow cytometer

Three types of microspheres were analyzed using the Apogee A50 nanoscale flow cytometer. Silica beads were purchased from Apogee FlowSystems Inc. (110, 179, 235, 304, 585, 880 nm). Latex beads were diluted 1:10 000 before being analyzed on the flow cytometer and came in sizes 100, 200, 500, and 1 μm (TetraSpeck beads, Invitrogen, Waltham, MA). Liposomes were generously provided by Dr. Jason Townson with sizes in 50, 100, 200, and 800 nm. (Sandia Institute). Liposomes were diluted 1:10 000× before being analyzed by the A50-Micro nanoscale flow cytometer.

2.3 | Preparation of extracellular vesicles from cultured cells

Both LnCap and PC-3M-LN4 cells were grown to 90% confluency in RPMI + 10% FBS cell culture media. Cells were harvested using 0.05% Trypsin + EDTA, and centrifuged at 200*g*'s for 5 min. The resultant cell pellet was then resuspended in water and left at room temperature for 1 h to allow EV release. The supernatant was reserved and submitted to one round of centrifugation at 1000*g*'s for 15 min at room temperature. This subsequent supernatant was reserved and used for experiments.

2.4 | Nanoscale flow cytometric detection of extracellular vesicles

To detect exosomes on the A50-Micro nanoscale flow cytometer, 20 μL of plasma was incubated with 1 μL of CD63-FITC (BD Biosciences; CA#561924), CD9-FITC (BD Biosciences; CA#555371), CD81-APC pre-conjugated antibody (BD Biosciences; CA# 656154), and/or anti-PSMA antibody (3E7 clone[12,21]) for 30 min at room temperature in the dark. Corresponding negative isotype controls, mouse IgG-FITC and mouse IgG-PE were added separately and used in exactly the same incubation conditions. Gates for each microparticle population were established by analyzing the isotype control first, modifying the gains for each PMT as necessary, and then analyzing the antibody labeled samples.

2.5 | Immunofluorescence staining of PC-3M-LN4 cells

PC-3M-LN4 cells (cultured to 90% confluency) were incubated on a 6-well plate overnight, at 37°C. Cells were fixed with 10% formalin for 10 min before blocking. Cells were incubated with 10% normal goat serum for an hour to block unspecific binding of antibody. To stain CD9 antigens on plasma membranes, cells were incubated with the diluted monoclonal CD9-FITC antibody in 10% normal goat serum overnight at room temperature in the dark. To label plasma membranes and nuclei of cells, cells were incubated with the diluted wheat germ agglutinin (Invitrogen) and Hoechst (Invitrogen) in 10% normal goat serum and PBS, respectively, for 5 min at room temperature in the dark.

3 | RESULTS

3.1 | Nanoscale flow cytometry can accurately resolve particles within the submicron size range

To determine the efficiency of the nanoscale flow cytometer in the analysis of submicron-sized particles, we calibrated the instrument using various silica calibration beads, latex beads and liposomes of known sizes. The nanoscale flow cytometer was calibrated by measuring the particle size of silica beads in the range of 110, 179, 235, 304, 585, 880, and 1300 nm (Figure 1A). The analysis of latex/polypropylene beads with various sizes (100, 200, 500, and 1000 nm) demonstrated polystyrene beads as small as 100 nm could be readily detected into discrete populations corresponding to each size group (Figure 1B). However, the A50-Micro nanoscale flow cytometer erred by positioning smaller polystyrene beads above larger silica beads in the LALS versus SALS sizing scatterplot (500 nm and 1 μm polystyrene beads over 880 nm and 1300 nm silica beads), revealing that different refractive indices of nanoparticles result in discrepant size measurements, with the polypropylene bead unsuitable for nFC due to its higher refractive index of 1.665 ± 0.046 and solid core compared to the vacant cores of silica nanoparticles and refractive index of 1.447 ± 0.021.[22] Blood borne EVs have been reported to have a refractive index range of 1.34-1.50.[22] Given the errors in measuring sizes regarding to material properties of beads and to evaluate the effectiveness of nanoscale flow cytometry in the enumeration of biological particles, we also analyzed liposomes of 50, 100, 200, and 800 nm in size (refractive index of 1.40). Liposomes of various sizes were readily distinguished (Figure 1C). The A50-Micro was even able to detect 50 nm liposomes, which gathered near the 100 nm level. As shown, the overlapped liposome distribution area between 50 and 100 nm suggests that the A50 might not have sufficient resolving power to distinguish liposomes with diameters less than 100 nm (Figure 1C).

3.2 | Exosome specific antibodies alone are a minor source of background noise

Removal of background noise, which is occasionally observed after immunofluorescent staining, is critical to improve efficient enumeration of fluorescently conjugated EVs. We examined the proportion of background events in samples of PBS alone and each fluorescently conjugated exosome specific antibody alone when resuspended in PBS diluent (CD63-FITC, CD9-FITC, and CD81-APC). PBS itself contained very low amounts of unidentified events mainly ranging from 100 to 200 nm with little fluorescent signal in the three channels of interest (Figure 2D). When we analyzed CD63-FITC and CD9-FITC in PBS respectively with a dilution index of 30, minimal contaminants in a range of 100 nm-300 nm were detected in both samples with a similar distribution pattern (Figures 2A and 2B). We detected fewer contaminating events sized ~100 nm in CD81-APC antibody only sample (Figure 2C, left panel). Meanwhile, we found a small population of ~200 nm sized

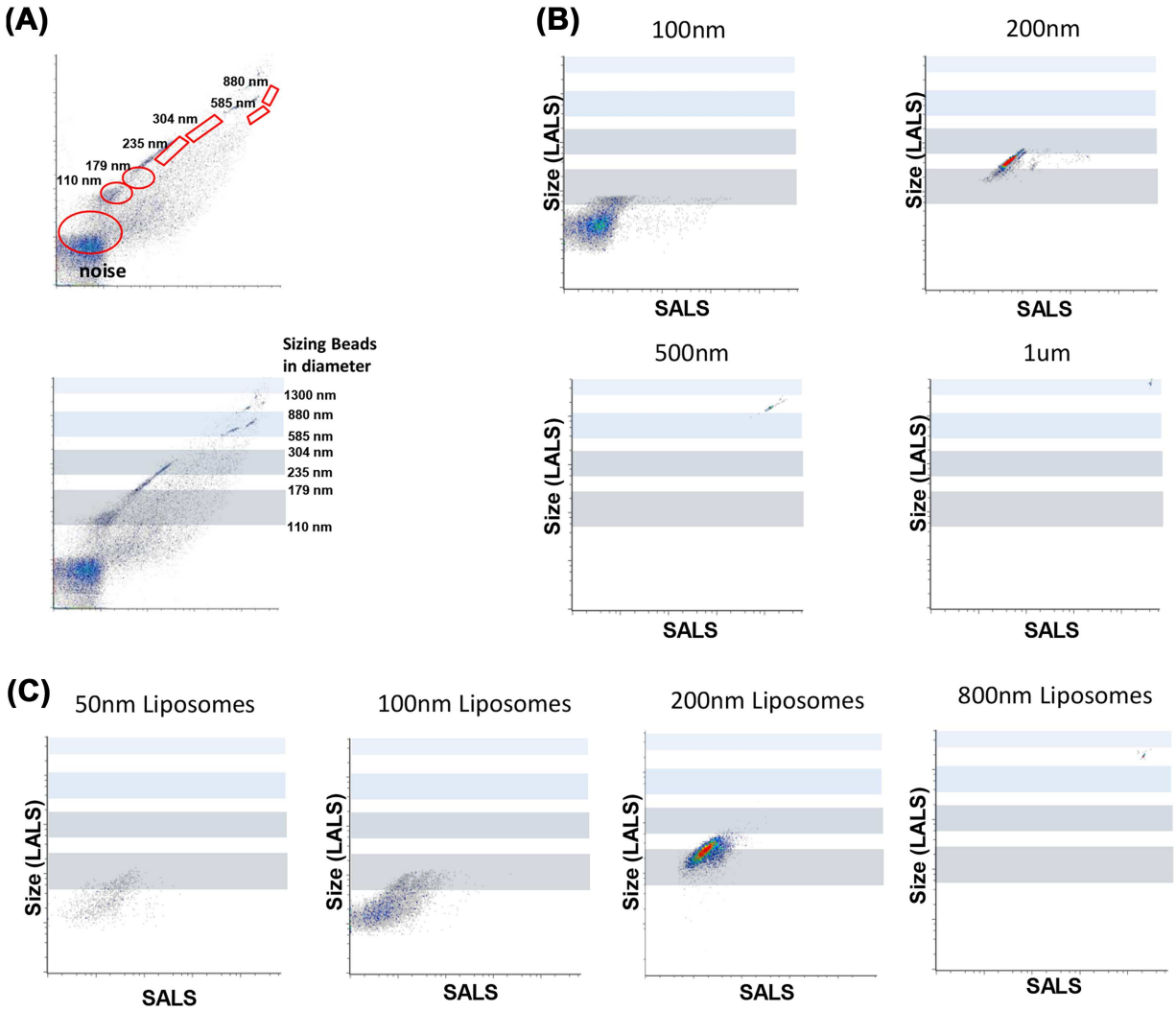

FIGURE 1 The Apogee A50-Micro nanoscale flow cytometer is able to readily analyze events within the submicron range. The analysis of silica calibration beads of various diameters, 110, 179, 235, 304, 585, 880, and 1300 nm (A), as well as latex/polystyrene beads of the diameters 100, 200, 500, and 1000 nm (B), show that the A50-Micro can resolve particles as small as 100 nm in size. The A50-Micro instrument is also able to accurately analyze microspheres with a lipid bilayer, as demonstrated by the analysis of liposomes that are 50, 100, 200, and 800 nm in size (C). [Color figure can be viewed at wileyonlinelibrary.com]

events producing high fluorescence intensity in the CD63-FITC antibody only sample (Figure 2A). CD9-FITC positive particles were also detected but the fluorescence intensity was much lower than that of the CD63-FITC antibody only sample (Figure 2B) while only few CD81-APC positive particles with fluorescence intensity were observed (Figure 2C, right panel). Hence, exosome specific antibodies (CD9-FITC, CD63-FITC, and CD81-APC) exhibited minimal non-specific binding and were used for immunofluorescent staining of exosomes in plasma samples.

3.3 | Nanoscale flow cytometry of antibody labeled patient plasma samples

To demonstrate that we could detect EVs within the nanoscale size range in human plasma samples, we analyzed unlabeled plasma samples from localized prostate cancer patients with the nFC. We detected a large number of events ranging from 50 nm to >1 um with the majority of events <500 nm in size (Figure 3A, top panel). The degree of background auto-fluorescence in all three fluorescent channels, which were 488nm-Green channel (Figure 3A, second panel), 488 nm-Orange channel (Figure 3A, third panel) and 639nm-Red channel (Figure 3A, bottom panel) was negligible. Of note, the 488-Orange channel detected minimal auto-fluorescence; whereas the 639-Red channel revealed more auto-fluorescence from larger sized EVs (>500 nm).

We next wanted to exclude the possibility that we are measuring albumin as EVs, which is the most abundant protein in human plasma and a potential source of artefact in our analysis. The analysis of high-concentration (7.5 mg/mL) BSA (Figure 3B) and low-concentration (0.45 mg/mL) BSA (Figure 3C) showed similar size distributions of nanoparticles at human plasma samples containing diluted BSA and the number of events was proportional

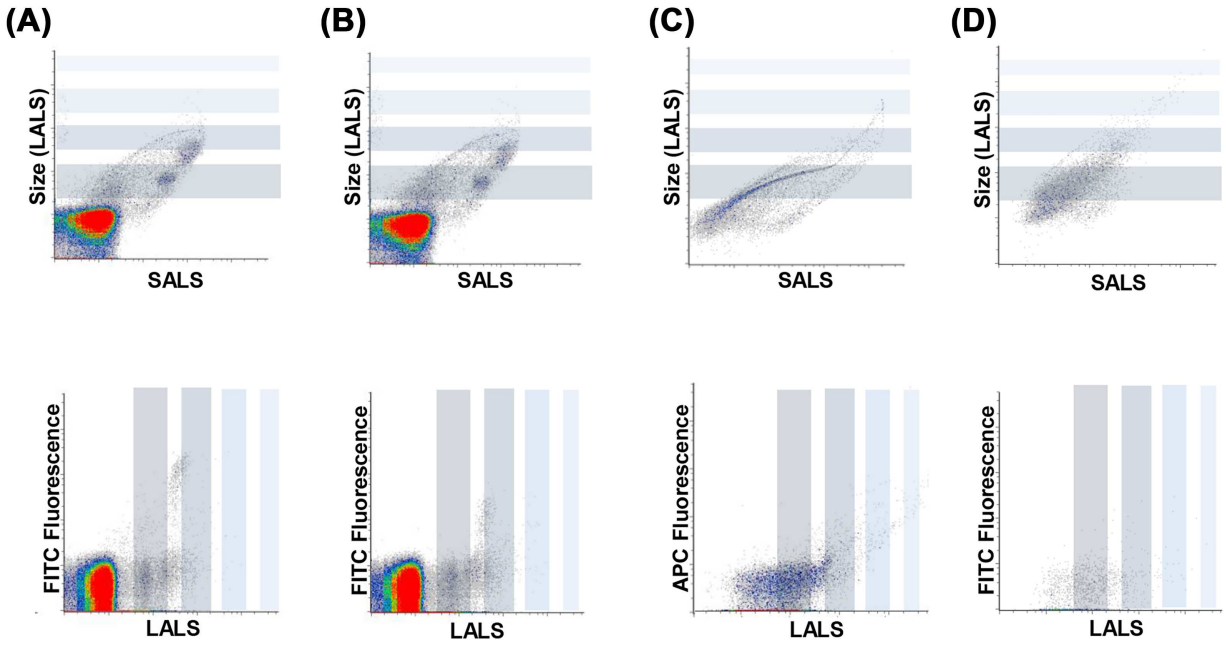

FIGURE 2 Anti-exosomal antibodies alone reveal minimal background during nFC. Analyses of CD63-FITC (A), CD9-FITC (B), and CD81-APC (C) antibodies, diluted into DPBS, show minimal particle contamination, as well as low levels of auto-fluorescence (top and bottom panels, respectively). Analysis of PBS, the diluent for all samples, shows minimal contaminating particles and fluorescent signal (D). [Color figure can be viewed at wileyonlinelibrary.com]

to the concentration of albumin (normal range of albumin in human plasma: 36-48 mg/mL). We subsequently analyzed the auto-fluorescence of BSA in concentrations of 7.5 mg/mL and 0.45 mg/mL at the three channels (488-Green channel, 488-Orange channel, and 639-Red channel). Minimal autofluorescence was detected in BSA. However, the size measurement of nano-particles in both high concentration and low concentration BSA samples was inconsistent in all channels. All events in albumin-high samples were <100 nm in terms of size according to the 639-Red channel, while events ranged between 100 and 500 nm in the 488-Green and Orange channel (Figures 3B and 3C). These results suggest that the 639-Red channel is not suitable for accurate sizing of EVs in the LALS versus SALS sizing scatterplot.

3.4 | Exosome markers on EVs in human plasma

Healthy volunteer patient plasma samples were immunostained with monoclonal antibodies against three exosome-specific antigens (CD9, CD63, CD81). CD9 positive EVs were observed in greatest abundance (Figure 4A, top left panel) with a broad size range of 50-600 nm (Figure 4A, bottom left panel, red rectangle). CD63 positive EVs were also present (Figure 4B, top left panel) in the size range of 200-600 nm but were not as abundant as CD9 positive EVs (Figure 4B, bottom left panel). CD81 antigens were absent on EVs in healthy patient plasmas (Figure 4C).

Prostate cancer patient plasma samples were also immunostained with exosome specific antigens (CD9, CD63, CD81). CD9-positive EVs were the most abundant in prostate cancer patient plasma samples (Figure 4A, top right panel) with a broad size range of 50-600 nm (Figure 4A, bottom right panel). CD63-positive EVs were also present (Figure 4B, top right panel) in the size range of 200-600 nm but not as abundant as CD9-positive EVs (Figure 4B, right panel). CD81 positive EVs were notably absent in prostate cancer patient plasma samples. EVs from healthy/prostate cancer patient plasmas showed the same degree of CD9/CD63 positivity without CD81 (Figure 4C), suggesting that the CD9 antigen is broadly present on different types of EVs including exosomes which are smaller than 150 nm in diameter. EV size-restricted expression of CD63 also reveals that large EVs (>200 nm) express CD63 on the surface.

3.5 | Exosome markers and the prostate specific membrane antigen biomarker on EVs from cultured prostate cancer cells

PC-3M-LN4 prostate cancer cells were stained with the exosomal markers CD9 and CD63 with wheat germ agglutinin used to define the cell surface membranes of unpermeabilized PC-3M-LN4 cells. An abundance of CD9 was observed (green signal) on the cell surface (Figure 5A), thus confirming that CD9 is a suitable surface antigen of prostate cancer cells and EVs generated by these cells as determined previously by others.[23] EVs from PC-3M-LN4 and LnCap cells were immunostained with CD9-FITC and CD63-FITC antibodies. EVs released from PC-3M-LN4 were highly CD9-FITC positive (Figure 5B, first panel). CD63 positive PC-3M-LN4 microparticles were also abundant as shown in Figure 5C (left panel). When EVs were gated on CD9/CD63 positivity, the size distribution of CD9-FITC positive microparticles (50-1000 nm) was similar to those of CD63-

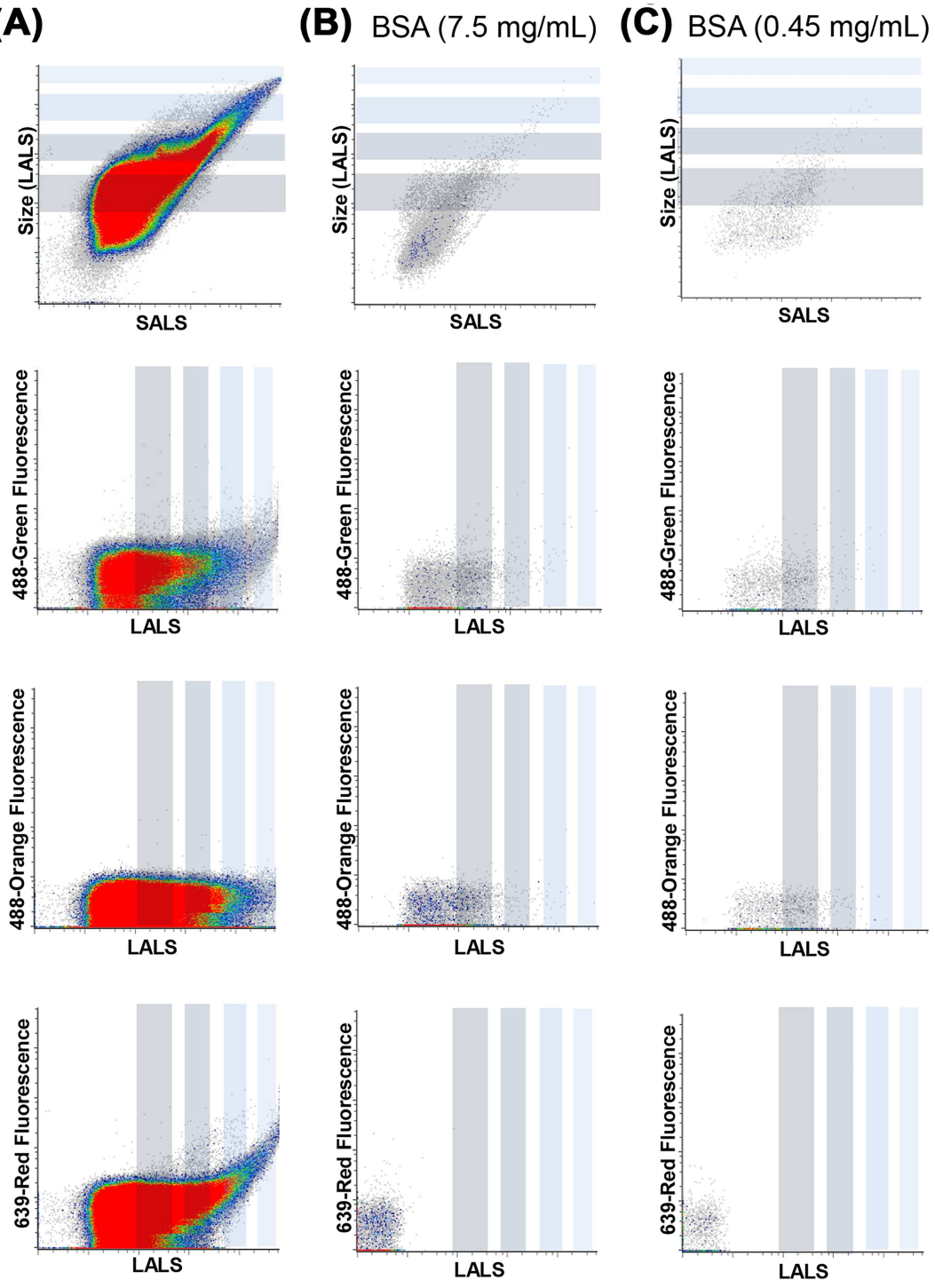

FIGURE 3 Minimal autofluorescence of EVs in patient plasma samples. Analysis of localized prostate cancer patient plasma by nFC (A, top panel) results in a wide size distribution of particles, with events ranging from 50 nm all the way to >1 um. Additionally, there is very little auto-fluorescence from the plasma alone in the 488-Green channel (second panel), 488-Orange channel (third panel), and 639-Red channel (bottom panel). Analysis of high-concentration (7.5 mg/mL) BSA (B) and low concentration (0.45 mg/mL) BSA (C), show minimal presence of EVs, as well as minimal florescence activity in each channel. [Color figure can be viewed at wileyonlinelibrary.com]

FITC positive microparticles (Figures 5B and 5C, second panel). We also detected a small subpopulation of EVs that were both PSMA-PE and CD9-FITC positive, exhibiting a size distribution of 200-1000 nm (Figure 5B, third and fourth panel). CD63 and PSMA-PE dual positive PC-3M-LN4 microparticles were also in low abundance and the size distribution was same as those in CD9 and PSMA dual positive microparticles (Figure 5C, third and fourth panel). EVs that were dual positive for exosome markers and PMSA were relatively rare (Yellow

rectangles represent the finding that CD9/CD63 & PSMA dual-positive PC-3M-LN4 microparticles were less than 20% of PSMA-positive microparticles).

LnCap EVs were stained with CD9-FITC and CD63-FITC and CD9 + CD63 dual positive EVs were less abundant compared to EVs generated by PC-3M-LN4 cells but continued to exhibit the same size distribution as PC-3M-LN4 generated EVs (Figures 5D and 5E, first and second panel). CD9/CD63 and PSMA dual positive EVs were also lower in proportion compared to PSMA-PE only EVs (Yellow rectangles represent that CD9/CD63 & PSMA dual positive LnCap microparticles were less than 10% of PSMA only positive microparticles) (Figures 5D and 5E, third panel). CD9/CD63 and PSMA dual positive LnCap microparticles exhibited a similar size distribution to those observed in PC-3M-LN4 generated EVs (200-1000 nm) (Figures 5D and 5E, fourth panel). Taken together, these results suggest that PSMA is not consistently co-expressed with exosome markers (CD9, CD63) on prostate derived EVs.

3.6 | Exosome markers and prostate specific membrane antigens on EVs from prostate cancer patient plasmas

nFC of PCa patient plasmas was performed to determine the proportion of prostate derived exosomes (<150 nm and co-expression of PSMA and CD9/CD63) and the proportion of prostate derived microparticles/microvesicles (>150 nm and co-expression of PSMA and CD9/CD63). Analysis of patient plasmas with antibodies specific for PSMA-PE (Figure 6A), CD9-FITC (Figure 6B), CD63-FITC (Figure 6C) positive EVs was performed with healthy volunteer plasma samples, prostate cancer patient (Gleason Score 3 + 3) plasma samples and prostate cancer patient (Gleason Score ≥4 + 4) plasma samples. The number of samples chosen was based on central limit theorem for powering groups based on a Gaussian distribution of data.

Nanoscale flow cytometry analysis of one plasma sample (ID PMP 087, Gleason Score 3 + 3) revealed (Figures 6A and 6B, left and middle panel) a large amount of both PSMA positive microparticles and CD9 positive microparticles (Figures 6A and 6B, far right graphs). Plasmas from Gleason Score 6 prostate cancer patients revealed more PSMA positive events when compared to Gleason Score ≥4 + 4 patients, but this did not reach statistical significance (Figure 6A, right panel). CD63 positive microparticles were comparatively fewer in number and concentration, with a narrower size range of 200-600 nm (Figure 6C, right panel) than CD9 positive microparticles and those of micro-particles released by prostate cancer cells in vitro (Figure 5, left panel and second panel). Meanwhile, healthy volunteer plasmas showed the least number of CD9 positive events among the three patient plasma sample groups.

Human plasma samples co-stained with antibodies specific for PSMA and exosome markers (CD9/CD63) revealed a small subpopulation of PSMA + CD9 dual positive EVs that exhibited a wide size range of 100-1000 nm (Figure 6D). The number of EVs that co-express PSMA + CD63 and was also examined in the same samples revealing a similar number and size distribution as was observed in the PSMA + CD9 dual positive EVs (Figure 6E). This finding suggests that PSMA positive EVs in human plasma seldom express exosome biomarkers such as CD9 and CD63. Comparison of the number of PSMA + CD9/CD63 EVs between different plasma sample groups revealed that low grade prostate cancer patient (Gleason Score 3 + 3) plasmas contained the most dual-positive EVs

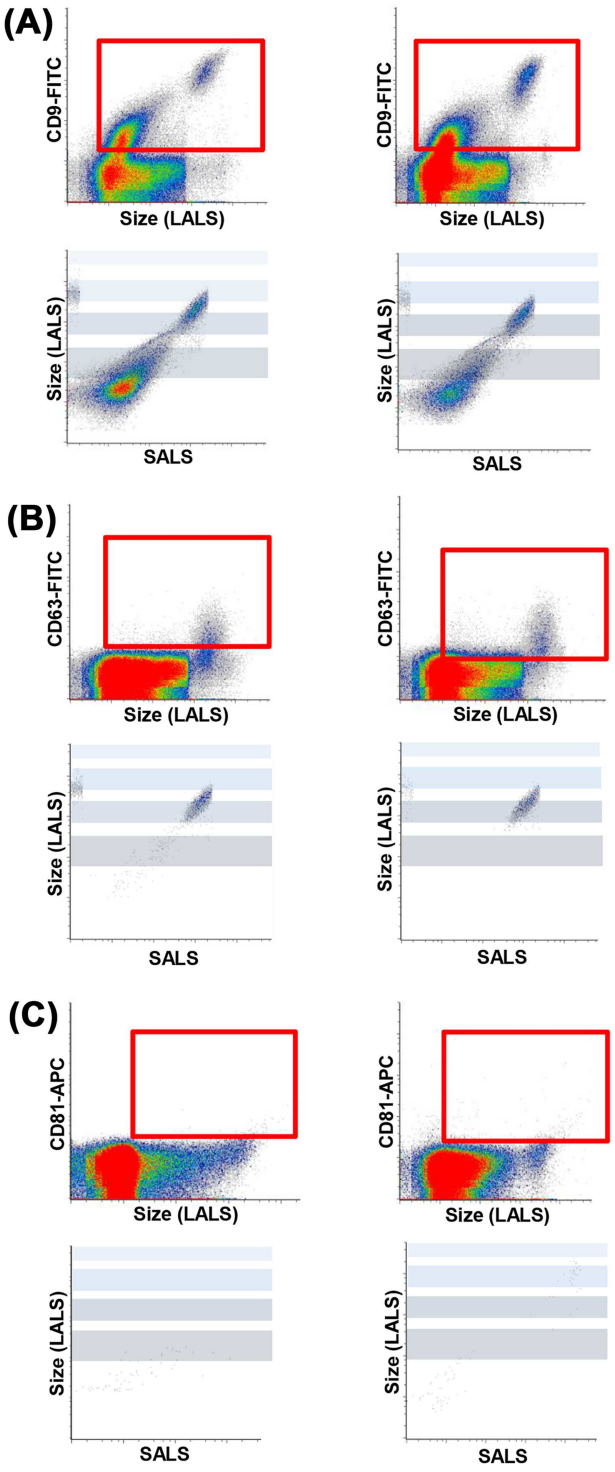

FIGURE 4 Continued.

regardless of exosomal marker used but this did not reach statistical significance. The lowest level of dual positive events were detected in plasma samples from high-risk prostate cancer patients (Gleason Score ≥4 + 4) (Figure 6D & 6E, right panel) but this did not reach statistical significance.

Table 1 summarizes the proportion of prostate derived EVs that express both an exosomal marker (CD9 top table, CD63 bottom table) and PSMA. There was no statistically significant difference between the three patient groups in terms of the proportion of dual positive EVs compared to total PSMA events (CD9/CD63&PSMA dual + ve/PSMA + ve). However, the proportion of dual + ve EVs in relation to total PSMA EV events was significantly higher in the CD9 table (12.5% to 19.1%) compared to CD63 (0.17% to 0.31%). This would suggest that CD9 is a superior EV marker than CD63.

4 | DISCUSSION

The use of exosomal markers such as CD9 and CD63 and CD81 are expected to help identify exosomes (50-150 nm) against larger EVs such as microparticles/microvesicles (>150 nm). In prostate cancer and normal prostatic epithelium, both exosomes and prostasomes/microparticles/microvesicles are produced and released into semen and blood respectively but a multi-parametric and high-throughput means of making this distinction was not possible until now. The use of nanoscale flow cytometry for prostate EV analysis as pioneered by our laboratory group sought to address the longstanding issue of the origin of prostate derived EVs as being released by exocytosis as exosomes, or if they were released at the cell membrane as microparticles/microvesicles. This method overcomes conventional means of EV analysis because nFC ascertains the antigen profile of each individual EV whereas other methods rely on batch analyses (ELISA, western immunoblotting) which incur contaminant EVs such as platelet microparticles. Our results reveal that the majority of prostate derived EVs are not exosomal in origin, but rather due to release at the cell membrane as occurs in platelets and endothelial cells. In fact, very few PSMA + ve EV events at the 100-150 nm analytical size range expressed either CD9 or CD63. The large majority of CD9 + ve prostate derived EVs were much larger in size, which was the same regardless of cancer grade (low vs high).

FIGURE 4 Exosome markers on microparticle-sized events in human plasma. Healthy volunteer patient plasma and localized prostate cancer patient plasma were stained with three exosomal markers, and analyzed with the A50-Micro nFC instrument. It was demonstrated that CD9 (A) and CD63 (B) were abundant in both healthy volunteer patient (left panels) and localized prostate cancer patient plasmas (right panels), whereas CD81 expressing EVs was absent (C). These populations are outlined in the regions of interest (red rectangles). Events staining positively for CD63 revealed a size range of 200-600 nm (B, bottom panels). In contrast, events staining positively for CD9 had a wider distribution of 50-600 nm (4A, top panels). [Color figure can be viewed at wileyonlinelibrary.com]

The lack of CD9/CD63 expression on PSMA + ve EVs brings into question their validity for identifying cancer EVs particularly prostate-derived exosomes if used alone or in combination with other exosomal markers. Given that we observed a small proportion of PSMA + ve EVs co-expressing CD9/CD63 (12-19% of PSMA + ve EVs in prostate cancer patients), exclusive use of CD9 and/or CD63 to determine cancer EV concentration in plasma would be erroneous. There are several limitations with this study related to the use of CD9/CD63 antibodies; there is no consensus clone for each antibody that is recommended by ISEV but the clone used in these experiments has been validated by various commercial entities and its effectiveness for immunostaining CD9 on cells and EVs is well documented.[24–27] Another limitation to consider is that PSMA itself is not purely prostate epithelium specific although its TPM (Transcripts of target per million total transcripts) for tissue specific expression is the highest in the prostate and liver.[28] We have determined previously that PSMA is indeed specific for prostate derived extracellular vesicles regardless of tumor grade or Gleason Score and that is why it was used as the tissue-specific marker in this study.[12] Lastly, the nFC instrument used in this study has an official analytical limit of analyzing 100 nm EVs in diameter but as seen in Figure 1C, it is still able to identify 50 nm liposomes albeit in an inefficient manner. This analysis does fully cover the exosome range (50-150 nm) and the microparticle/microvesicle range (150-1000 nm) and while some EVs of the exosomal range may not be fully captured, at least a portion of those EVs were included in our analysis.

nFC is ideal for enumerating EVs in a multi-parametric manner, meaning that it is able to determine if an individual EV expresses one target of interest or multiple targets. Much like conventional flow cytometry, nFC can use the same fluorophores without any limit to the number of targets being analyzed. In these experiments, two targets were of focus, one representing an exosomal marker (CD9 or CD63) and the second target representing a tissue-specific marker (PSMA). In our studies, CD81 did not have utility in identifying exosomes nor did it bind to any similar magnitude as CD9 or CD63 on larger EVs. In the same vein, CD9 proved to be a more "ubiquitous" exosomal marker whereas CD63 was observed in significantly lower numbers of EVs and PSMA + ve EVs. This may be due to the fact that mRNA levels of CD9 (841.3 TPM) are higher than CD63 levels (682.8 TPM) in the prostate (www.proteinatlas.org).[28] However, CD81 levels are also high in the prostate (835.7 TPM). It behooves other investigators to first consult this online resource to determine if CD9/CD63/CD81 levels are abundant in their tissue of interest prior to experimentation.

The primary finding of this work is that prostate derived EVs do not all express exosomal markers such as CD9/CD63/CD81. This has two main implications, in that EV release in prostate cancer and normal prostatic epithelium occurs on the cell membrane, which means that other cell surface biomarkers can be used to develop more effective and accurate "liquid biopsies." The other implication is that prostate derived EV release is triggered by non-exocytotic mechanisms as one

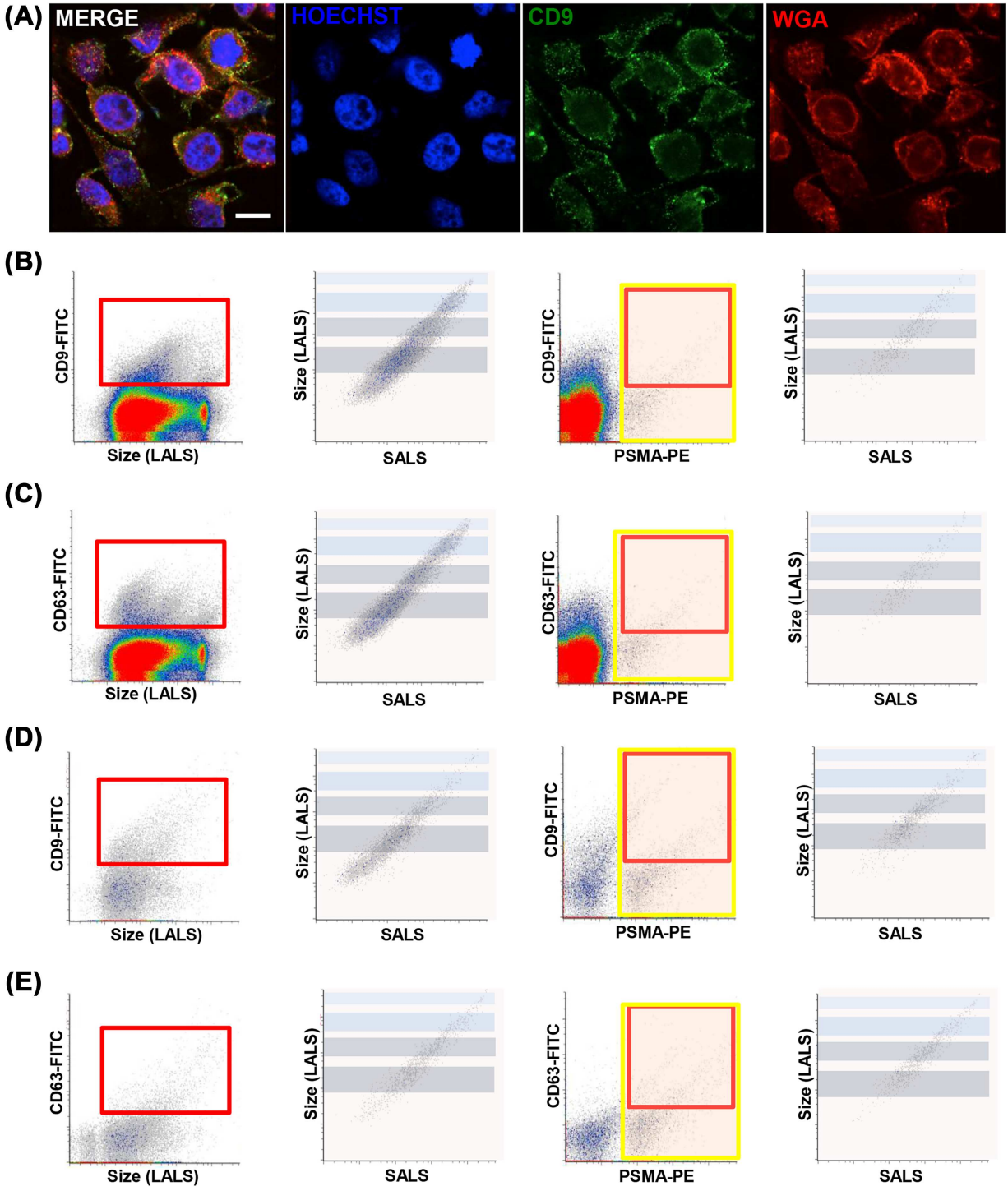

FIGURE 5 Exosome markers and Prostate Specific Membrane Antigen on EVs generated from various prostate cancer cell lines. Immunofluorescent staining of PC-3M-LN4 cells with CD9-FITC antibody revealed abundant cell surface localization as demarcated by wheat germ agglutinin-Alexa594 staining (A). PC-3M-LN4 EVs reveal a high abundance of CD9 + ve EVs (B, left panel) as indicated by the red rectangle. When the EVs are gated on CD9 positivity, they reveal a wide size distribution from 50 to 1000 nm (B, second panel). EVs staining positively for both PSMA and CD9 are less abundant (B, third panel, red rectangle) but have a narrower size distribution of 250-1000 nm (B, right panel). PC-3M-LN4 EVs stained with CD63-FITC and PSMA-PE revealed similar results (C). LNCaP EVs stained with CD9-FITC and PSMA-PE revealed a lower overall abundance of EV events, as well as a lower number of CD9 + ve EVs (D, left panel, red rectangle). When gated on CD9 positivity; however, EVs show a higher concentration of events in the 50-500 nm range (D, second panel). Events that are dual positive for CD63 and PSMA are low (D, third panel, red rectangle) and show a similar size distribution to those in PC-3M-LN4 EVs (D, right panel). LnCap EVs stained with CD63-FITC and PSMA-PE reveal a CD63 positive population (E, left panel, red rectangle) that has a larger size (E, second panel). Evaluation of CD63 and PSMA dual positive populations reveal similar results to the PC-3M-LN4 microparticles (E, third and right panels). [Color figure can be viewed at wileyonlinelibrary.com]

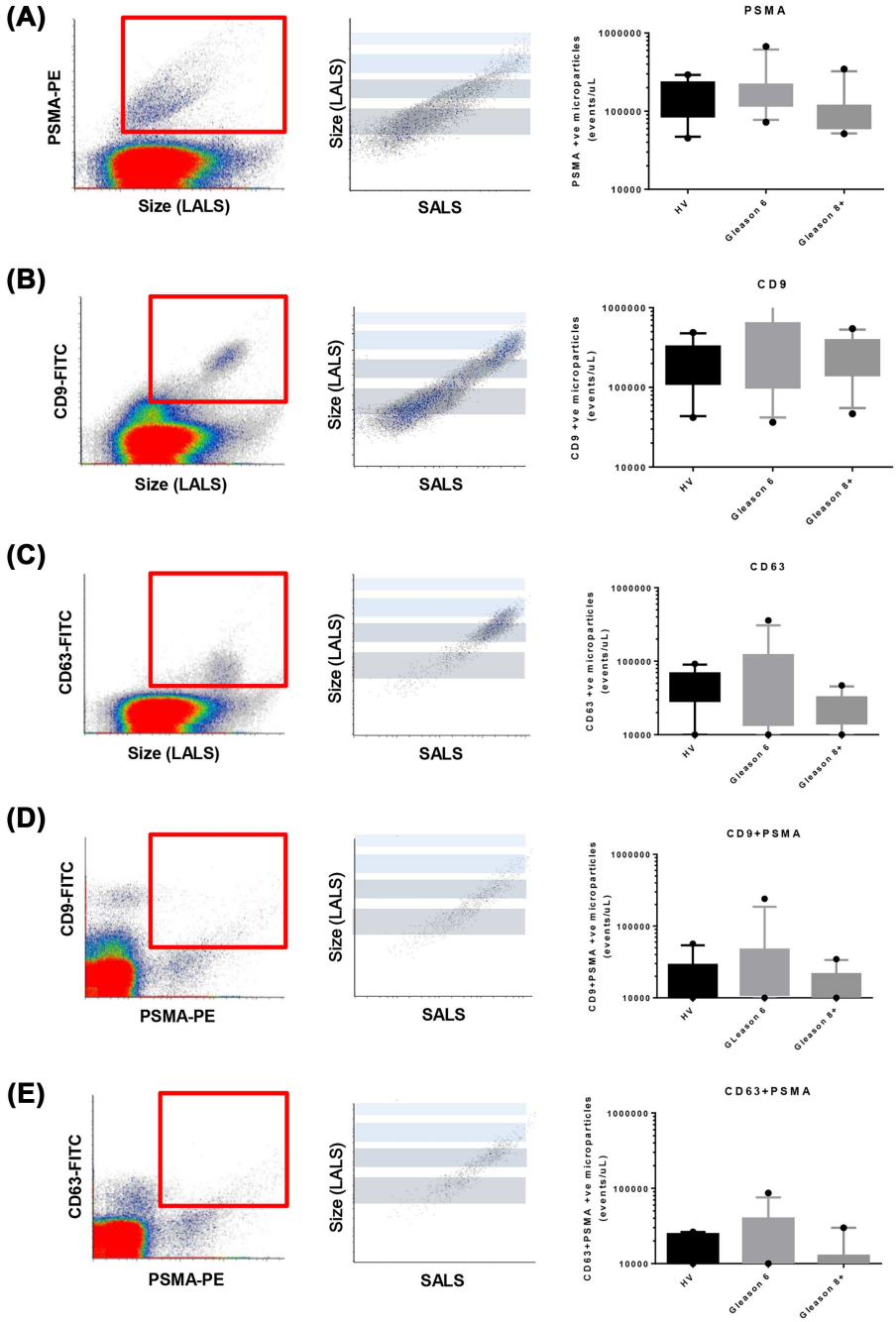

FIGURE 6 nFC analysis of prostate cancer patient plasmas for prostate-derived EVs that express exosomal markers. Patient plasma samples revealed a large amount of PSMA positive (A) and CD9 positive (B) microparticles (red gates, left panels). Both of the gated microparticles distribute from 50 to 1000 nm in size (A and B, second from left panels). Meanwhile, CD63 positive microparticles were less abundant (C) revealing a size range of 200-600 nm. Events that are dual positive for CD9 and PSMA are in low abundance (D, left panel, red gate) and have a wide size distribution of 100-1000 nm (D, middle panel). Evaluation of CD63 and PSMA dual positive populations reveal similar results to CD9 and PSMA dual positive populations (E). Prostate cancer patient (Gleason Score 3 + 3) plasma samples revealed the most positive events in all staining strategies (right panels), while least positive events were detected in prostate cancer patient (Gleason Score ≥4 + 4) plasma samples except staining with CD9-FITC (B, right panel). [Color figure can be viewed at wileyonlinelibrary.com]

would expect with exosomes. Instead, EV release by prostate cancer cells is likely due to apoptosis, necroptosis, necrosis, migration, or other cell activation types. These translational results have significant bearing on how the biology of EVs produced by cancer can be used to deduce tumor cell function in the patient. In this case, prostate derived EVs present in low and high grade disease were released by dying tumor cells or cells undergoing migration while a small proportion of these EVs were simply released due to the constitutive exocytotic nature of prostate epithelium releasing prostasomes into the seminal fluid or blood.

TABLE 1 Enumeration of Various EVs Bearing PSMA and Exosomal Markers

Group	CD9+ve EVs (events/uL)	PSMA+ve EVs (events/uL)	CD9&PSMA dual+ve (events/uL)	CD9&PSMA dual+ve /PSMA+ve (%)
CD9 Exosome Marker				
HV (n = 10)	217782 ± 44247	165067 ± 26979	20733.7 ± 4795	12.5 ± 2.4%
GS 3 + 3 (n = 12)	456809 ± 146265	225841 ± 55625	43165 ± 20402	19.1 ± 4.1%
GS≥4 + 4 (n = 10)	279241 ± 46701	111252 ± 27313	15045 ± 2827	13.5 ± 2.2%
CD63 Exosome Marker				
HV (n = 10)	52046 ± 8486	169253 ± 27736	14739 ± 2497	0.31 ± 0.14%
GS 3 + 3 (n = 12)	75548 ± 33377	228312 ± 60550	25828 ± 7592	0.28 ± 0.13%
GS≥4 + 4 (n = 10)	23653 ± 3643	94223 ± 17917	16697 ± 2275	0.17 ± 0.04%

ACKNOWLEDGMENTS

HSL is supported by a Movember/Prostate Cancer Canada Rising Star Award (#RS2012-008 and #RS2016-56) and received operating grant support by the Prostate Cancer Fight Foundation. KD is supported by a Chinese Government Scholarship.

CONFLICTS OF INTEREST

None of the authors have any conflicts to declare.

ORCID

Hon S. Leong http://orcid.org/0000-0001-7801-1402

REFERENCES

1. Ronquist GK, Larsson A, Stavreus-Evers A, Ronquist G. Prostasomes are heterogeneous regarding size and appearance but affiliated to one DNA-containing exosome family. *Prostate*. 2012;72:1736–1745.
2. Ronquist KG, Ek B, Stavreus-Evers A, Larsson A, Ronquist G. Human prostasomes express glycolytic enzymes with capacity for ATP production. *Am J Physiol Endocrinol Metab*. 2013;304:E576–E582.
3. Tavoosidana G, Ronquist G, Darmanis S, et al. Multiple recognition assay reveals prostasomes as promising plasma biomarkers for prostate cancer. *Proc Natl Acad Sci USA*. 2011;108:8809–8814.
4. Utleg AG, Yi EC, Xie T, et al. Proteomic analysis of human prostasomes. *Prostate*. 2003;56:150–161.
5. Aalberts M, van Dissel-Emiliani FMF, van Adrichem NPH, et al. Identification of distinct populations of prostasomes that differentially express prostate stem cell antigen, annexin A1, and GLIPR2 in humans. *Biol Reprod*. 2012;86:82.
6. Zhang H, Freitas D, Kim HS, et al. Identification of distinct nanoparticles and subsets of extracellular vesicles by asymmetric flow field-flow fractionation. *Nat Cell Biol*. 2018;20:332–343.
7. Sahlén GE, Egevad L, Ahlander A, Norlén BJ, Ronquist G, Nilsson BO. Ultrastructure of the secretion of prostasomes from benign and malignant epithelial cells in the prostate. *Prostate*. 2002;53:192–199.
8. Nawaz M, Camussi G, Valadi H, et al. The emerging role of extracellular vesicles as biomarkers for urogenital cancers. *Nat Rev Urol*. 2014;11:688–701.
9. Principe S, Jones EE, Kim Y, et al. In-depth proteomic analyses of exosomes isolated from expressed prostatic secretions in urine. *Proteomics*. 2013;13:1667–1671.
10. Hosseini-Beheshti E, Pham S, Adomat H, Li N, Tomlinson Guns ES. Exosomes as biomarker enriched microvesicles: characterization of exosomal proteins derived from a panel of prostate cell lines with distinct AR phenotypes. *Mol Cell Proteomics*. 2012;11:863–885.
11. Minciacchi VR, Freeman MR, Di Vizio D. Extracellular vesicles in cancer: exosomes, microvesicles and the emerging role of large oncosomes. *Semin Cell Dev Biol*. 2015;40:41–51.
12. Biggs CN, Siddiqui KM, Al-Zahrani AA, et al. Prostate extracellular vesicles in patient plasma as a liquid biopsy platform for prostate cancer using nanoscale flow cytometry. *Oncotarget*. 2016;7:8839–8849.
13. Velonas VM, Woo HH, dos Remedios CG, Assinder SJ. Current status of biomarkers for prostate cancer. *Int J Mol Sci*. 2013;14:11034–11060.
14. Lu Q, Zhang J, Allison R, et al. Identification of extracellular delta-catenin accumulation for prostate cancer detection. *Prostate*. 2009;69:411–418.
15. Taylor BS, Pal M, Yu J, et al. Humoral response profiling reveals pathways to prostate cancer progression. *Mol Cell Proteomics*. 2008;7:600–611.
16. Prensner JR, Rubin MA, Wei JT, Chinnaiyan AM. Beyond PSA: the next generation of prostate cancer biomarkers. *Sci Transl Med*. 2012;4:127rv3.
17. Gomes J, Lucien F, Cooper TT, et al. Analytical considerations in nanoscale flow cytometry of extracellular vesicles to achieve data linearity. *Thromb Haemost*. 2018;118:1612–1624.
18. Xiao D, Ohlendorf J, Chen Y, Taylor DD, Rai SN, Waigel S, et al. Identifying mRNA, microRNA and protein profiles of melanoma exosomes. *PLoS ONE*. 2012;7:e46874.
19. Vojtech L, Woo S, Hughes S, et al. Exosomes in human semen carry a distinctive repertoire of small non-coding RNAs with potential regulatory functions. *Nucleic Acids Res*. 2014;42:7290–7304.
20. Minciacchi VR, You S, Spinelli C, et al. Large oncosomes contain distinct protein cargo and represent a separate functional class of tumor-derived extracellular vesicles. *Oncotarget*. 2015;6:11327–11341.
21. Wolf P, Freudenberg N, Bühler P, et al. Three conformational antibodies specific for different PSMA epitopes are promising diagnostic and therapeutic tools for prostate cancer. *Prostate*. 2010;70:562–569.

22. van der Pol E, Coumans FA, Sturk A, Nieuwland R, van Leeuwen TG. Refractive index determination of nanoparticles in suspension using nanoparticle tracking analysis. *Nano Lett*. 2014;14:6195–6201.
23. Espenel C, Margeat E, Dosset P, et al. Single-molecule analysis of CD9 dynamics and partitioning reveals multiple modes of interaction in the tetraspanin web. *J Cell Biol*. 2008;182:765–776.
24. Higginbotham JN, Zhang Q, Jeppesen DK, et al. Identification and characterization of EGF receptor in individual exosomes by fluorescence-activated vesicle sorting. *J Extracell Vesicles*. 2016;5:29254.
25. Koliha N, Wiencek Y, Heider U, et al. A novel multiplex bead-based platform highlights the diversity of extracellular vesicles. *J Extracell Vesicles*. 2016;5:29975.
26. Oksvold MP, Neurauter A, Pedersen KW. Magnetic bead-based isolation of exosomes. *Methods Mol Biol*. 2015;1218:465–481.
27. Crescitelli R, Lässer C, Szabó TG, et al. Distinct RNA profiles in subpopulations of extracellular vesicles: apoptotic bodies, microvesicles and exosomes. *J Extracell Vesicles*. 2013;2.
28. Uhlén M, Fagerberg L, Hallström BM, et al. Proteomics. Tissue-based map of the human proteome. *Science*. 2015;347:1260419.

How to cite this article: Padda RS, Deng FK, Brett SI, et al. Nanoscale flow cytometry to distinguish subpopulations of prostate extracellular vesicles in patient plasma. *The Prostate*. 2019;1–12. https://doi.org/10.1002/pros.23764